J|A|C|S
ARTICLES
Published on Web 11/22/2005

Generalized Anomeric Interpretation of the "High-Energy" N−P Bond in *N*-Methyl-*N*′-phosphorylguanidine: Importance of Reinforcing Stereoelectronic Effects in "High-Energy" Phosphoester Bonds

Eliza A. Ruben,[†] Michael S. Chapman,*[,†,£] and Jeffrey D. Evanseck*[,‡]

Contribution from the Institute of Molecular Biophysics, and Department of Chemistry and Biochemistry, Florida State University, Tallahassee, Florida 32306, and Center for Computational Sciences and the Department of Chemistry and Biochemistry, Duquesne University, 600 Forbes Ave, Pittsburgh, Pennsylvania 15282

Received July 14, 2005; E-mail: evanseck@duq.edu; chapman@sb.fsu.edu.

Abstract: Electronic structure calculations have been performed on a model *N*-phosphorylguanidine, or phosphagen, to understand the stereoelectronic factors contributing to the lability of the "high-energy" N−P bond. The lability of the N−P bond is central to the physiological role of phosphagens involving phosphoryl transfer reactions important in cellular energy buffering and metabolism. Eight protonated forms of *N*-methyl-*N*′-phosphorylguanidine have been energy minimized at levels of theory ranging up to B3LYP/6-311++G(d,p) and MP2/6-311++G(d,p) to investigate the correlation between protonation state and N−P bond length. Selected forms have also been minimized using the CCSD/6-311++G(d,p) and QCISD/6-311++G(d,p) levels of theory. Bulk solvation energies using the polarized continuum model (PCM) with B3LYP/6-311++G(d,p) test the influence of the surroundings on computed structures and energies. The N−P bond length depends on the overall protonation state where increased protonation at the phosphoryl group or deprotonation at the unsubstituted N″ nitrogen results in shorter, stronger N−P bonds. Natural bond orbital analysis shows that the protonation state affects the N−P bond length by altering the magnitude of stabilizing n(O) → σ^*(N−P) stereoelectronic interactions and to a lesser extent the σ(N−P) → σ^*(C−N″) and σ(N−P) → σ^*(C−N) interactions. The computations do not provide evidence of a competition between the phosphoryl and guanidinium groups for the same lone pair on the bridging nitrogen, as previously suggested by opposing resonance theory. The computed n(O) → σ^*(N−P) anomeric effect provides a novel explanation of "high-energy" N−P bond lability. This offers new mechanistic insight into phosphoryl transfer reactions involving both phosphagens and other biochemically important "high-energy" phosphoester bonds.

Introduction

Phosphagens (*N*-phosphorylguanidines) are a group of small, phosphorylated biomolecules that participate in phosphoryl transfer reactions,[1−4] as shown in Figure 1.

Phosphoryl transfer reactions that break and form "high-energy" phosphoester bonds have been recently referred to as "the centerpiece of biochemical processes" due to their fundamental roles in metabolism and signaling.[5−9] The reversible transfer of the phosphoryl group from *N*-phosphorylguanidines to ADP is crucial in maintaining steady ATP concentrations.

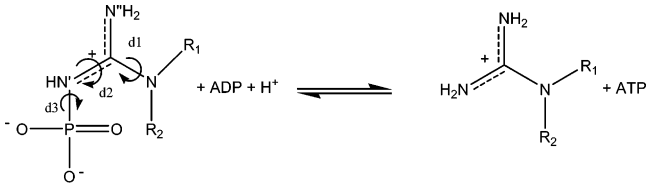

Figure 1. Schematic of the phosphagen reaction as modeled with *N*′-phosphorylguanidine. The designation of N, N′, and N″ for the guanidinium nitrogens is used throughout the text. The R_1 group of *N*′-phosphorylguanidine, which does not participate in the reaction, is modeled as a methyl group. In most *N*′-phosphorylguanidines, or phosphagens, R_2 = H except for creatine where $R_2 = CH_3$ (ref 1).

ATP is the currency from which most biological processes derive all their energy needs, and this reversible phosphoryl transfer is essential in tissues subject to rapid fluctuations in energy demands, such as the heart muscle[4] and nervous tissue.[10]

While crystallography,[11−16] biochemical kinetics,[14,16−19] and thermodynamic studies[20,21] have all furthered the understanding

[†] Institute of Molecular Biophysics, Florida State University.
[£] Department of Chemistry and Biochemistry, Florida State University.
[‡] Duquesne University.

(1) Eggleton, P.; Eggleton, G. P. *J. Physiol. (London)* **1927**, *63*.
(2) James, E.; Morrison, J. F. *Biochim. Biophys. Acta* **1966**, *128*, 327.
(3) Stucki, J. W. *Eur. J. Biochem.* **1980**, *109*, 257.
(4) Rossi, A. M.; Eppenberger, H. M.; Volpe, P.; Cotrufo, R.; Wallimann, T. *J. Biol. Chem.* **1990**, *265*, 5258.
(5) Dzeja, P. P.; Terzic, A. *J. Exp. Biol.* **2003**, *206*, 2039.
(6) Allen, K. N.; Dunaway-Mariano, D. *Trends Biochem. Sci.* **2004**, *29*, 495.
(7) Mildvan, A. S. *Proteins: Struct., Funct., Genet.* **1997**, *29*, 401.
(8) Knowles, J. R. *Ann. Rev. Biochem.* **1980**, *19*, 877.
(9) Dzeja, P. P.; Bortolon, R.; Perez-Terzic, C.; Holmuhamedov, E. L.; Terzic, A. *Proc. Natl. Acad. Sci. U.S.A.* **2002**, *99*, 10156.
(10) Lapin, E. P.; Weissbarth, S.; Maker, H. S.; Lehrer, G. M.; Weiss, C. *J. Neurosci. Res.* **1983**, *10*, 9.

of phosphagen kinase enzymes that catalyze the reaction in biological systems, critical molecular level aspects surrounding the chemistry of *N*-phosphorylguanidine substrates remain unknown. Among the needed studies is a clear understanding of the molecular origin of the labile or "high-energy" N′−P bond between the phosphoryl and guanidine groups.[22] The weakness of the N′−P bond is essential to the physiological role of phosphagens, where the exothermic cleavage of the N′−P bond is coupled to the endothermic formation of the O−P bond, thus enabling the favorable formation of ATP. The determinants of N′−P bond lability control the capacity of phosphagens in fulfilling their role in providing phosphoryl groups in ATP formation and to date have not been clearly defined nor quantified.

Both N′−P and O−P bonds have been described as labile or "high-energy" bonds because the hydrolysis of these bonds is accompanied by relatively large negative standard free energy change, ΔG^0. Traditionally, the term "high-energy bond" is not the same as "bond energy", which is defined as the energy required to break, not hydrolyze, a covalent bond.[23] The standard free energy change of ATP hydrolysis is ~ -7.3 kcal/mol and that of *N*′-phosphorylcreatine is ~ -10.3 kcal/mol, indicating a preference of O−P over N′−P bond formation. However under more complex physiological conditions, there is little difference in the overall free energy change.[23,24] Because both compounds exhibit relatively large negative free energy changes during hydrolysis,[23] the chemical rationalization of the "high-energy" character of the N′−P bond in *N*-phosphorylguanidines has been assumed implicitly to be similar to that of the O−P bond in ATP.[23,24] Because phosphoryl transfer involves the breaking or formation of "high-energy" phosphoryl bonds, the chemistry of these bonds has a profound effect on mechanism and catalysis.[6]

The "high-energy" character or weakness of the O−P phosphoanhydride bonds in ATP has been traditionally attributed to three main factors. First, resonance stabilization in the phosphoester reactant is less favorable than in the hydrolyzed products causing the O−P bond to be weakened.[23−26] Protonation states directly impact resonance stabilization and control of mechanism in phosphate monoesters.[27−29] Weaker resonance stabilization in the phosphodiester has been rationalized as an "opposing resonance effect" brought about by competition between adjacent, resonance stabilized, phosphoryl groups for the same lone pair on the bridging oxygen atom.[23,25,26,30−32] Second, electrostatic repulsion between negatively charged oxygen atoms on the adjacent phosphoryl groups destabilizes the esterified form and should lengthen the O−P bond.[23,24] The phosphagen guanidinium and phosphoryl groups are oppositely charged, so electrostatic repulsion does not contribute to the lability of the N′−P bond. Finally, solvation of ATP has been shown to be less favorable than that of its hydrolysis products.[23,24,33] Apart from solvation, these arguments have been qualitative.

Resonance factors, including opposing resonance theory, have been used to explain N′−P bond lability in *N*-phosphorylguanidines due to energetic similarity with O−P phosphoanhydride bonds in ATP.[23,25] However, there are no reports in the literature that directly examine the resonance factors governing the underlying weakness of the N′−P bond and subsequently its ability to affect phosphoryl transfer reactions or mechanism. One reason for this is that the weakness of the N′−P bond itself makes phosphagens in free acid forms difficult for experimentation. Indeed to the best of our knowledge, geometric parameters of phosphagens in isolation have not been reported.

Crystallographic studies of a phosphagen kinase enzyme, transition state analogue complex[11] suggests that the enzyme stabilizes a transient, hitherto unanticipated quaternary form of the phosphorylated N′ nitrogen. In phosphagen kinase enzymes, electrostatic calculations suggest that it is entirely conceivable that alternate protonated forms may exist.[14,15] Because protonation states influence conjugation and resonance, the reported electrostatic calculations emphasize the need for detailed studies of phosphagen structure and their determinants of stability. However, even if only one form predominates in biology, the aim of using the different forms in this is to probe any possible association between N′−P bond length and resonance through systematic investigation.

Due to the physiological importance and lack of understanding of the "high-energy" N′−P bond in significant biochemical reactions, a systematic study of N′−P bond lability has been undertaken. Computational methods have been utilized to study resonance and stereoelectronic effects of different protonation states upon the chemistry of the N′−P bond. Electronic structure calculations with a variety of basis sets and quantum chemical methods have been employed to investigate the structure and stability of the N′−P bond. Electronic structure methods with natural bond order analysis provide the necessary atomistic and stereoelectronic detail to identify and quantify the determinants of N′−P lability.

Computational Methods

All electronic structure calculations were carried out with the Gaussian program[34,35] using the computational resources at the FSU School for Computational Science and Information Technology (CSIT),

(11) Zhou, G.; Somasundaram, T.; Blanc, E.; Parthasarathy, G.; Ellington, W. R.; Chapman, M. S. *Proc. Natl. Acad. Sci. U.S.A.* **1998**, *95*, 8449.
(12) Yousef, M. S.; Fabiola, F.; Gattis, J. L.; Somasundaram, T.; Chapman, M. S. *Acta Crystallogr., Sect. D* **2002**, *58*, 2009.
(13) Yousef, M. S.; Clark, S. A.; Pruett, P. K.; Somasundaram, T.; Ellington, W. R.; Chapman, M. S. *Protein Sci.* **2003**, *12*, 103.
(14) Pruett, P. S.; Azzi, A.; Clark, S. A.; Yousef, M.; Gattis, J. L.; Somasundaram, T.; Ellington, W. R.; Chapman, M. S. *J. Biol. Chem.* **2003**, *29*, 26952.
(15) Gattis, J. L.; Ruben, E.; Fenley, M. O.; Ellington, W. R.; Chapman, M. S. *Biochemistry* **2004**, *43*, 8680.
(16) Azzi, A.; Clark, S. A.; Ellington, W. R.; Chapman, M. S. *Protein Sci.* **2004**, *13*, 575.
(17) Suzuki, T.; Tomoyuki, T.; Uda, K. *FEBS Lett.* **2003**, *533*, 95.
(18) Schlattner, U.; Forstner, M.; Eder, M.; Stachowiak, O.; Fritz-Wolf, K.; Wallimann, T. *Mol. Cell. Biochem.* **1998**, *184*, 125.
(19) Schlattner, U.; Eder, M.; Dolder, M.; Khuchua, Z. A.; Strauss, A. W.; Wallimann, T. *Biol. Chem.* **2000**, *381*, 1063.
(20) Teague, W. E. J.; Dobson, G. P. *J. Biol. Chem.* **1992**, *267*, 14084.
(21) Teague, W. E., Jr.; Dobson, G. P. *J. Biol. Chem.* **1999**, *274*, 22459.
(22) Throughout this text the N−P bond will be referred to as the N′−P bond, consistent with the atom definitions in Figure 1.
(23) Voet, D.; Voet, J. G. *Biochemistry*; John Wiley: New York, 2003.
(24) Berg, J.; Tymoczko, J. L.; Stryer, L. *Biochemistry*, 5th ed.; W. H. Freeman & Co.: New York, 2002.
(25) Kalckar, H. M. *Chem. Rev.* **1941**, *28*, 71.
(26) Oesper, P. *Arch. Biochem.* **1950**, *27*, 255.
(27) Akola, J.; Jones, R. O. *J. Phys. Chem. B* **2003**, *107*, 11774.
(28) Wilkie, J.; Gani, D. *J. Chem. Soc., Perkin Trans.* **1996**, *5*, 783.
(29) Grzyska, P. K.; Czyryca, P. G.; Purcell, J.; Hengge, A. C. *J. Am. Chem. Soc.* **2003**, *125*, 13106.
(30) de Meis, L. *Arch. Biochem. Biophys.* **1993**, *306*.
(31) Hayes, D. M.; Kenyon, G. L.; Kollman, P. A. *J. Am. Chem. Soc.* **1978**, *100*, 4331.
(32) Hill, T. L.; Morales, M. F. *J. Am. Chem. Soc.* **1951**, *73*, 1656.
(33) George, P.; Witonsky, R. J.; Trachtman, M.; Wu, C.; Dorwart, W.; Richman, L.; Richman, W.; Shurayh, F.; Lentz, B. *Biochim. Biophys. Acta* **1970**, *223*, 1.
(34) Frisch, M. J.; et al. *Gaussian 98*, revision A.9; Gaussian, Inc.: Pittsburgh, PA, 1998.

the Center for Computational Sciences[36] at Duquesne University, and the Pittsburgh Supercomputer Center.[37]

To identify reasonable, low-energy gas-phase conformations, the protonated systems were subjected to grid searches along the three main dihedrals, C−N−C−N″ (d1), N−C−N′−P (d2), and C−N′−P−O (d3), as shown in Figure 1. The dihedral angles were scanned in 30° increments from 0° to 180° using the PM3[38,39] semiempirical method. PM3 was chosen because of its ability to provide stationary points as a starting point for further optimizations at higher levels of theory for a variety of phosphorus and nitrogen containing compounds.[40,41] The energy-minimized structures were located using Hartree−Fock (HF), density functional theory (DFT), and second-order many-body Møller−Plesset[42] theory (MP2). Specifically, DFT was implemented by using Becke's three-parameter hybrid (exchange) functional[43] with gradient corrections provided by the Lee, Yang, and Parr[44] (B3LYP). Acknowledging the lack of dispersive forces in DFT methods,[45] MP2 optimizations were carried out on all structures to serve as a point of verification and test of DFT. To further validate the MP2 and B3LYP geometries and energies, two selected structures were optimized using coupled-cluster theory (CCSD)[46−48] and quadratic CI (QCISD).[49,50] The Pople style 3-21G,[51−53] 6-31G(d),[54−56] 6-31+G(d),[54−57] and 6-311++G-(d,p)[57−59] basis sets were utilized. Contributions due to thermal, vibrational, rotational, and translational motions, including zero-point energies, were included separately by standard statistical mechanical procedures available in Gaussian. Frequency analysis has been used to confirm all stationary points as minima or transition structures and provide thermodynamic and zero-point energy corrections.[60]

The PCM continuum solvation model,[61,62] which has been described in detail,[63−67] was used to probe the effect of solvent on each structure. Energy minimization has been carried out using the B3LYP/6-311++G(d,p) level of theory with dielectric constants of 78.39 and 2.379. Briefly in the PCM model, the solvent is treated as an infinite continuum of a specified dielectric. The solute or molecule is placed within a cavity defined as a series of interlocking van der Waals spheres centered on the atoms. The interaction between the solute and solvent, or free energy of solvation, is then calculated as a potential term added on to the molecular Hamiltonian. Specific to the PCM model, this potential term includes electrostatic, dispersive, and cavitation terms. Because self-consistency between the solute charge distribution and solvent reaction field is required to evaluate the amended Hamiltonian, this method is termed an SCRF or self-consistent reaction field method.

Natural bond order (NBO)[68] analysis was performed using the NBO 3.1 program[69] interfaced into the Gaussian program. NBO transforms the nonorthogonal atomic orbitals from the HF wave function into natural atomic orbitals (NAO), natural hybrid orbitals (NHO), and natural bond orbitals (NBO) each of which are complete and orthonormal. This allows electron density to be treated in a more intuitive manner, i.e., localized onto bonds and atoms, leading to a better description of the molecule as a localized Lewis structure. In effect, NBO transformation provides filled orbitals that are more concentrated (localized) in terms of occupancies. This then allows delocalizing interactions to be treated as a perturbation through second-order perturbation theory. The $E(2)$ energy values from the second-order perturbation method then provide a reasonable quantitative description of the magnitude of such delocalizing interactions.[70,71] The deletion method in NBO analysis is important to evaluate the possibility of anticooperative energy interactions and as a check of the computed $E(2)$ energy values.[71] However, the deletion method is currently implemented for only HF and DFT, and not for MP2. Consequently, the deletion method has been applied using both HF and DFT on all three sets of energy-minimized structures.

Results and Discussion

A two-step approach is used to identify the stereoelectronic effects responsible for the lability of the N′−P bond of *N*-phosphorylguanidines. First, through electronic structure calculations, clearly defined trends are established between the different protonation states and N′−P bond lengths, with N′−P bond lengths being the physical characteristic associated with N′−P lability. Second, using an NBO analysis of the different protonated forms, N′−P bond lengths are shown to depend on the delocalization and stereoelectronic interactions of phosphoryl and guanidinium groups.

Phosphagen Geometries and Energies. *N*-Methyl-*N*′-phosphorylguanidine is used as a model compound representative of phosphagens. The model contains atoms common to all phosphagens, but in this model, $R_1 = CH_3$ where the substituent in natural phosphagens is one of several groups from acetate to ethyl phosphoserine.[72−74] A total of five protonation sites (Figure 2) of *N*-methyl-*N*′-phosphorylguanidine, three of which are chemically identical (sites 1−3), have been investigated.

Of the nine possible geometries investigated (Figure 3), 16 low-energy configurations, two conformations each for **1b**−**3c**, have been selected from the grid searches at the PM3 level for further investigation. The difference between the first

(35) Frisch, M. J.; et al. *Gaussian 03*; revision A.1 ed.; Gaussian, Inc.: Pittsburgh, PA, 2003.
(36) Supported by the National Science Foundation (CHE-031147) and the U.S. Department of Education (P116Z040100 and P116Z050331).
(37) Supported by the National Science Foundation (AAB/PSC CHE-030008).
(38) Stewart, J. J. P. *J. Comput. Chem.* **1989**, *10*, 209.
(39) Stewart, J. J. P. *J. Comput. Chem.* **1989**, *10*, 221.
(40) Aviyente, V.; Houk, K. N. *J. Phys. Chem. A* **2001**, *105*, 383.
(41) Cooney, K. D.; Cundari, T. R.; Hoffman, N. W.; Pittard, K. A.; Temple, M. D.; Zhao, Y. *J. Am. Chem. Soc.* **2003**, *125*, 4318.
(42) Møller, C.; Plesset, M. S. *Phys. Rev.* **1934**, *46*, 618.
(43) Becke, A. D. *Phys. Rev. A* **1988**, *38*, 3098.
(44) Lee, C.; Yang, W.; Parr, R. G. *Phys. Rev. B* **1988**, *37*, 785.
(45) Byrd, E. F. C.; Scuseria, G. E.; Chabalowski, C. F. *J. Phys. Chem. B* **2004**, *108*, 13100.
(46) Cizek, J. *J. Chem. Phys.* **1966**, *45*, 4256.
(47) Cizek, J. *Adv. Chem. Phys.* **1969**, *14*, 35.
(48) Scuseria, G. E.; Janssen, C. L.; Schaefer, H. F. *J. Chem. Phys.* **1988**, *89*.
(49) Scuseria, G. E.; Schaefer, H. F. *J. Chem. Phys.* **1989**, *90*, 3700.
(50) Gauss, J.; Cramer, C. *Chem. Phys. Lett.* **1988**, *150*, 280.
(51) Salter, E. A.; Trucks, G. W.; Bartlett, R. J. *J. Chem. Phys.* **1989**, *90*.
(52) Binkley, J. S.; Pople, J. A.; Hehre, W. J. *J. Am. Chem. Soc.* **1980**, *102*, 939.
(53) Gordon, M. S.; Binkley, J. S.; Pople, J. A.; Pietro, W. J.; Hehre, W. J. *J. Am. Chem. Soc.* **1982**, *104*, 2797.
(54) Binkley, J. S.; Pople, J. A.; Pietro, W. J.; Hehre, W. J. *J. Am. Chem. Soc.* **1982**, *104*, 2797.
(55) Hehre, W. J.; Ditchfield, R.; Pople, J. A. *J. Chem. Phys.* **1972**, *56*, 2257.
(56) Dill, J. D.; Pople, J. A. *J. Chem. Phys.* **1975**, *62*, 2921.
(57) Francl, M. M.; Pietro, W. J.; Hehre, W. J.; Binkley, J. S.; Gordon, M. S.; Defrees, D. J.; Pople, J. A. *J. Chem. Phys.* **1982**, *77*, 3654.
(58) Clark, T.; Chandrasekhar, J.; Spitznagel, G. W.; Schleyer, P. v. R. *J. Comput. Chem.* **1983**, *4*, 294.
(59) Krishnan, R.; Binkley, J. S.; Seeger, R.; Pople, J. A. *J. Chem. Phys.* **1980**, *72*, 650.
(60) Acevedo, O.; Evanseck, J. D. Transition States and Transition Structures. In *Computational Medicinal Chemistry for Drug Discovery*; Bultinck, P., De Winter, H., Langenaeker, W., Tollenaere, J. P., Dekker, M., Eds.; Marcel and Dekker: New York, 2004; p 323.
(61) Miertus, S.; Scrocco, E.; Tomasi, J. *Chem. Phys.* **1981**, *55*, 117.
(62) Miertus, S.; Tomasi, J. *Chem. Phys.* **1982**, *65*, 239.
(63) Morao, I.; McNamara, J. P.; Hillier, I. H. *J. Am. Chem. Soc.* **2003**, *125* (3), 628−629; **2003**, *125*, 628.
(64) Cances, E.; Mennucci, B.; Tomasi, J. *J. Chem. Phys.* **1997**, *107*, 3032.
(65) Tomasi, J.; Rersico, M. *Chem. Rev.* **1994**, *94*, 2027.
(66) Iron, M. A.; Martin, J. M. L.; van der Boom, M. E. *J. Am. Chem. Soc.* **2003**, *125*, 11702.
(67) Freccero, M.; Di Valentin, C.; Sarzi-Amade, M. *J. Am. Chem. Soc.* **2003**, *125*, 3544.
(68) Reed, A. E.; Weinhold, F.; Curtiss, L. A.; Pochatko, D. J. *J. Chem. Phys.* **1986**, *84*, 5687.
(69) Glendening, E. D.; Reed, A. E.; Carpenter, J. E.; Weinhold, F. *NBO*, Version 3.1, Theoretical Chemistry Institute, University of Wisconsin, Madison, 1995.
(70) Alabugin, I. V.; Zeidan, T. A. *J. Am. Chem. Soc.* **2002**, *124*, 3175.
(71) Alabugin, I. V.; Manoharan, M.; Zeidan, T. A. *J. Am. Chem. Soc.* **2003**, *125*, 14014.
(72) van Thoai, N. J.; Roche, J. *Ann. N. Y. Acad. Sci.* **1960**, *90*, 923.
(73) Eggleton, P.; Eggleton, G. P. *Biochem. J.* **1927**, *21*, 190.
(74) Ennor, A. H.; Morrison, J. F. *Physiol. Rev.* **1958**, *38*, 631.

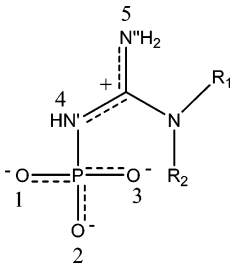

Figure 2. *N*-Methyl-*N*′-phosphorylguanidine with protonation sites labeled 1 through 5. The designation of N, N′, and N″ used in the text is shown.

and second lowest energy structure is in all cases a 180° rotation about the dihedral labeled d2 in Figure 1. The energy difference between the two low-energy structures is less than 1.0 kcal/mol at the PM3 level. Where a third low conformation is found, the energy difference between the second and third lowest energy structures is at least 6.0 kcal/mol, so these higher energy conformations are not further considered.

The remaining 16 low-energy structures have been further energy minimized at levels of theory ranging from HF/3-21G to B3LYP/6-311++G(d,p). At the B3LYP/6-311++G(d,p) level, the energy difference between the d2 rotamers increases to at least 7.0 kcal/mol. Therefore, only the lower energy *E*-forms have been further optimized using MP2/6-311++G(d,p). The computed N′−P bond lengths are given in Tables 1 and 2. Selected phosphagen bond lengths are given in Table S1 in the Supporting Information. Relative energies of the final eight structures are given in Table 3. There are no imaginary frequencies for any of the eight structures indicating that each structure is a true minimum.

Validation of acceptable quantum chemical methods and basis sets is complicated by the lack of prior theoretical calculations and the limited experimental information available. The only experimental structure comes from a crystal of the hydrated sodium salt of *N*-phosphorylcreatine.[75] Its relevance here is limited by the substitution of $R_2 = CH_3$ in creatine instead of $R_2 = H$ in other phosphagens. This affects the C−N bond length and delocalizing interactions involving C−N′ and C−N″. Second, the coordination of the Na^+ counterions to the phosphoryl group affects the O−P bond lengths relative to the free acid forms from the computations.

The computations are validated by comparing structures and energies with results from higher levels of theory. The CCSD/6-311++G(d,p) and QCISD/6-311++G(d,p) levels of theory have been selected as the standards, since they have been shown to produce accurate structures and relative energies.[76−78] The N′−P bond of both isomers of **1a** dissociates during energy minimization attempts using all levels of theory employed. Isomers of **2a** also dissociate during energy minimization using MP2/6-311++G(d,p), CCSD/6-311++G(d,p), and QCISD/6-311++G(d,p). However, all other levels of theory give a stationary point for **2a**. Even though minima are located, it is clear that the lower levels of theory do not predict a stabilized structure, since the N′−P bonds are longer than 2.0 Å (Table 1).

With differences in **2a** between levels of theory, it was important to validate the MP2/6-311++G(d,p) and B3LYP/6-311++G(d,p) methods for the other structures. The energy-minimized structures of **2b** are compared with those computed at CCSD/6-311++G(d,p) and QCISD/6-311++G(d,p). As seen in Table 2, the MP2 and B3LYP N′−P bond lengths show little change with the higher levels of theory. With the use of the 6-311++G(d,p) basis set, the difference in the N′−P bond lengths between MP2 and CCSD is 0.008 Å, whereas the difference is 0.006 Å between MP2 and QCISD for structure **2b**. Overall across selected bond lengths as given in Table 2, the difference when comparing MP2 with CCSD and QCISD is 0.004 ± 0.003 Å and 0.004 ± 0.002 Å, respectively. Consequently, MP2/6-311++G(d,p) is found to produce structures in solid agreement with those of both CCSD/6-311++G(d,p) and QCISD/6-311++G(d,p). B3LYP/6-311++G(d,p) is also in strong agreement with the higher levels of theory (Table 2).

Fully optimized structures together with N′−P bond lengths at both the B3LYP/6-311++G(d,p) and MP2/6-311++G(d,p) are shown in Figure 4. B3LYP produces geometric results that are close to MP2 when using the 6-311++G(d,p) basis set for all structures (Table 1 and Table S1 in the Supporting Information) except **2a** (where B3LYP predicts a stationary point). In fact, the computed average energy difference is 0.5 ± 0.2 kcal/mol between MP2/6-311++G(d,p)//MP2/6-311++G(d,p) and MP2/6-311++G(d,p)//B3LYP/6-311++G(d,p) across all computed structures (Table 3). Most importantly, all levels of theory show bond lengths that are correlated, i.e., all bond lengths change from structure to structure in similar ways. For example, the N′−P bond length always decreases in the following order: **1b** > **3a** > **1c** > **2b** > **3b** > **2c** > **3c** for all levels of theory.

To probe the effect of solvent on the structures, optimizations were performed on all structures using the PCM method in toluene (dielectric constant, 2.379) and water (dielectric constant, 78.39). The structures show that with increasing dielectric constant, the N′−P bond length shortens with no difference in the trends between N′−P bond lengths and anomeric energies (shown in Figures 7 and 9).

Stereoelectronic and Anomeric Effects. The weakness of the N′−P bond has been traditionally explained by the increased resonance stability of the dissociated phosphoryl and guanidinium groups compared to that of the *N*-phosphorylguanidine product.[23−26] The framework for increased resonance stability has been given by opposing resonance theory,[23,25,26] where the phosphoryl and guanidinium groups compete for the same lone pair on the bridging nitrogen, N′, giving a weakened N′−P bond (Figure 5).

By changing the protonation states of *N*-methyl-*N*′-phosphorylguanidine, investigation of the relationship between increased resonance at the phosphoryl and guanidinium groups and N′−P bond lengths, as well as testing opposing resonance theory, is possible. By examining the amount of electron delocalization from the lone pair on the N′ to the guanidinium and phosphoryl groups using an NBO analysis, we obtain a quantitative estimate of the extent to which competition for the lone pair on N′ is correlated with N′−P bond lengths. Specifically, through second-order perturbation methods, an NBO analysis quantifies the interactions between Lewis and non-Lewis type NBOs, showing how much the actual delocalized system deviates from the idealized Lewis structure. Second-order perturbation energy terms provide a quantitative estimate of the delocalizing

(75) Herriott, J. R.; Love, W. E. *Acta Crystallogr., Sect. B* **1968**, *24*, 1014.
(76) Byrd, E. F. C.; Sherrill, C. D.; Head-Gordon, M. *J. Phys. Chem. A* **2001**, *105*, 9736.
(77) Pu, J.; Truhlar, D. G. *J. Phys. Chem. A* **2005**, *109*, 773.
(78) Sheng, Y.; Leszczynski, J. *J. Phys. Chem. A* **2002**, *106*, 12095.

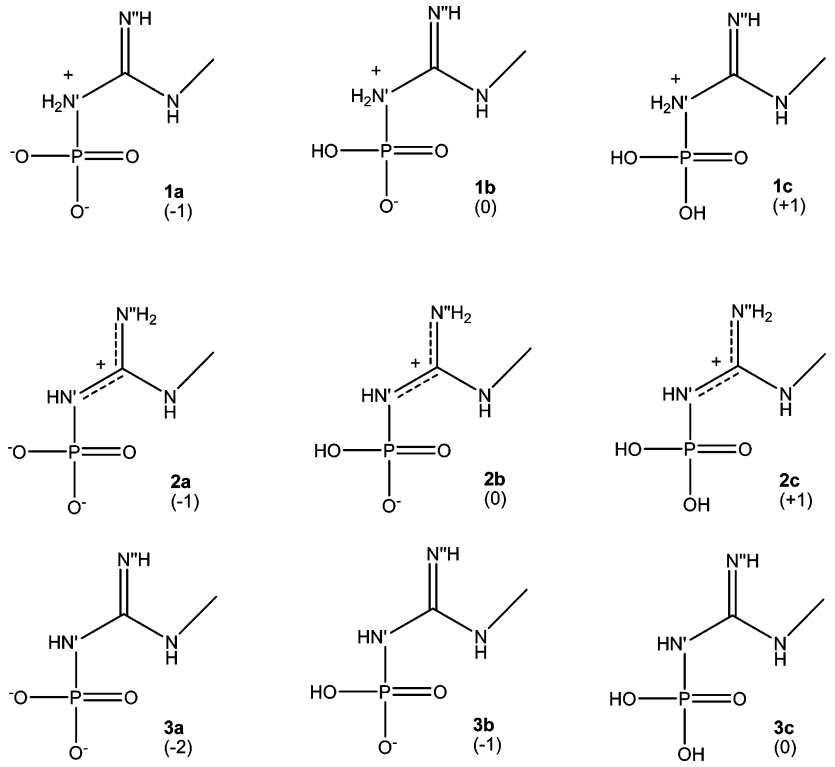

Figure 3. The nine structures studied in this work. Overall charges are given in parentheses.

Table 1. N′−P Bond Lengths Calculated at Different Levels of Theory

	HF/6-31G(d)	HF/6-31+G(d)	HF/6-311++G(d,p)	B3LYP/6-31G(d)	B3LYP/6-31+G(d)	B3LYP/6-311++G(d,p)	MP2/6-311++G(d,p)
1b	1.947	1.940	1.938	2.007	1.998	2.007	1.979
1c	1.802	1.803	1.796	1.836	1.837	1.830	1.823
2a	2.055	2.004	2.004	2.014	2.021	2.010	nd
2b	1.796	1.788	1.784	1.831	1.821	1.821	1.816
2c	1.701	1.699	1.694	1.722	1.721	1.717	1.710
3a	1.845	1.831	1.825	1.883	1.870	1.870	1.856
3b	1.718	1.715	1.711	1.742	1.740	1.737	1.737
3c	1.658	1.658	1.654	1.676	1.677	1.673	1.673

Table 2. Structural Comparison of **2b** at High Levels of Theory[a]

structure **2b**	B3LYP/ 6-311++G(d, p)	MP2/ 6-311++G(d, p)	CCSD/ 6-311++G(d, p)	QCISD/ 6-311++G(d, p)
N′−P	1.821	1.816	1.808	1.810
P−O1	1.636	1.629	1.624	1.624
P−O2	1.477	1.476	1.469	1.471
P−O3	1.508	1.507	1.498	1.500
C−N′	1.335	1.335	1.333	1.334
C−N″	1.362	1.369	1.369	1.371
C−N	1.329	1.327	1.327	1.328

[a] Average error between B3LYP and CCSD = 0.007 ± 0.003 Å; average error between B3LYP and QCISD = 0.007 ± 0.004 Å; average error between MP2 and CCSD = 0.004 ± 0.003 Å; average error between MP2 and QCISD = 0.004 ± 0.002 Å.

Table 3. Relative Energy Differences (between Structures) Calculated by the Various Methods Including Scaled ZPE[a,b]

level of theory	1b–2b	1c–2c	1b–3c	2b–3c	2a–3b
HF/6-31G(d)	25.6	55.1	19.8	−5.8	28.5
HF/6-31+G(d)	25.4	54.2	19.1	−6.2	27.5
HF/6-311++G(d,p)	26.2	54.7	23.0	−3.3	29.9
B3LYP/6-31G(d)	20.7	46.4	11.6	−9.1	20.1
B3LYP/6-31+G(d)	20.3	45.6	10.6	−9.6	19.8
B3LYP/6-311++G(d,p)	21.2	46.0	13.6	−7.6	20.7
MP2/6-311++G(d,p)	17.3	42.4	12.6	−4.7	nd
MP2/6-311++G(d,p)//HF/ 6-311++G(d,p)	18.1	43.6	13.8	−4.3	25.0
MP2/6-311++G(d,p)//B3LYP/ 6-311++G(d,p)	18.1	42.7	12.8	−5.3	23.4

[a] The scale factor used for the ZPE was 0.9135 for HF/6-31G(d), 0.9163 for HF/6-31+G(d) and HF/6-311++G(d,p), 0.9806 for all B3LYP calculations, and 0.9748 for MP2 calculations (ref 91). [b] Average error between MP2 and B3LYP = 2.9 ± 0.9 kcal/mol; average error between HF and B3LYP = 8.3 ± 3.4 kcal/mol; average error between MP2//MP2 and MP2//B3LYP = 0.5 ± 0.2 kcal/mol.

interactions. Therefore, NBO analysis provides a convenient method to identify and relate specific delocalization interactions with N′−P bond lengths.

Since the identity of the delocalizing interactions responsible for the trend in N′−P bond lengths are of interest, we focus on interactions with σ(N′−P) as a donor or with σ^*(N′−P) as an acceptor. Note that electron density loss from σ(N′−P) and electron density gain in σ^*(N′−P) both lead to longer, weaker N′−P bonds. The delocalization interaction responsible for the resonance form type A is identified as n(N′) → σ^*(C−N″) or n(N′) → σ^*(C−N), while that of type B is given by n(N′) → σ^*(P−O), as illustrated in Figure 5. We also focus on these interactions to investigate the correlation between N′−P bond length and the magnitude of such interactions, to test opposing resonance theory. These findings are presented below.

Role of Oxygen Lone Pairs in Destabilizing the N′−P Bond. The six structures, **2a** through **3c**, show distinct variations

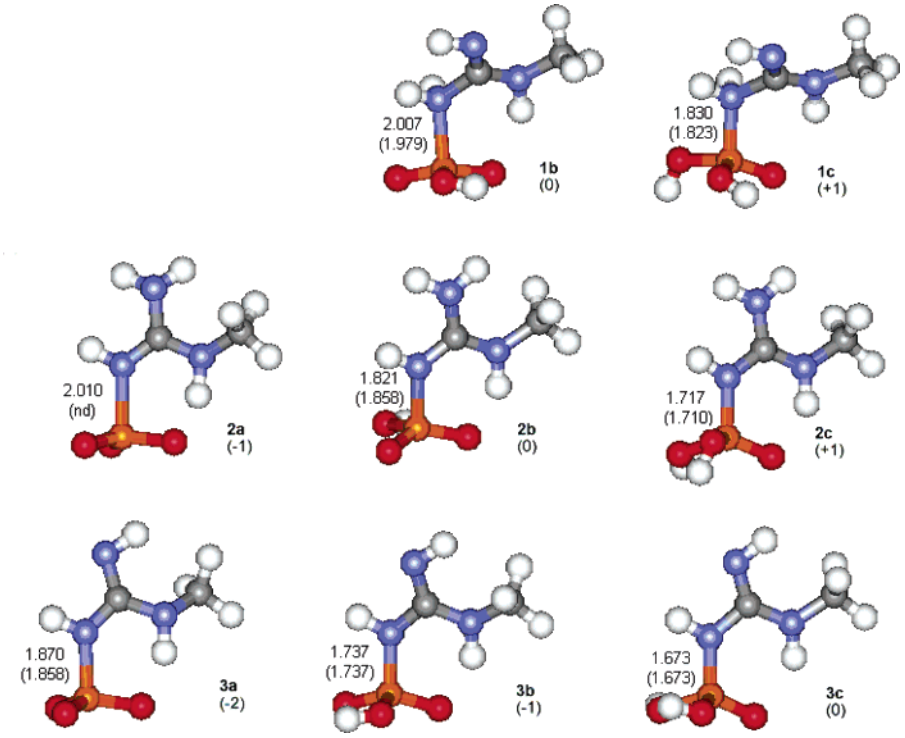

Figure 4. Eight optimized structures of *N*-methyl-*N*′-phosphorylguanidine. N′−P bond lengths in angstroms are given at the B3LYP/6-311++G(d,p) and MP2/6-311++G(d,p) levels (in parentheses). Selected bond lengths at different levels of theory are shown in Table S1 in the Supporting Information.

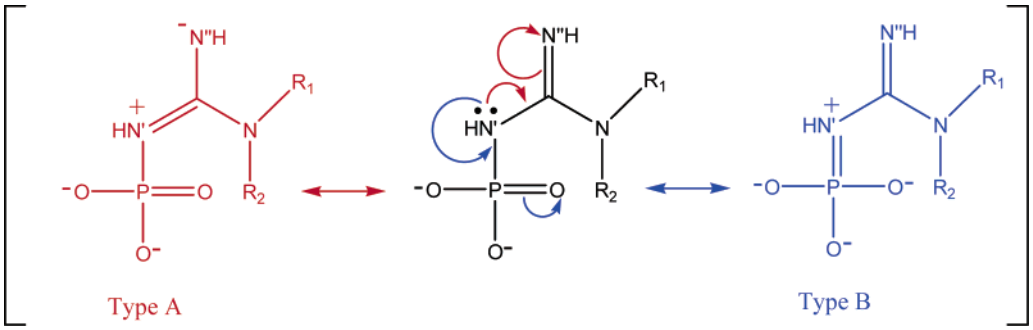

Figure 5. In opposing resonance theory, there are two types of resonance forms, type A and type B. It has been proposed that both types compete for the same lone pair on the bridging nitrogen, N′. As a result, the N′−P bond is weakened (refs 18−21). In NBO nomenclature, the delocalization interaction responsible for type A is identified as n(N′) → σ^*(C−N″) or n(N′) → σ^*(C−N) and type B is identified as an n(N′) → σ^*(P−O) orbital interaction.

in N′−P bond lengths (Table 1, Figure 4). Two trends can be seen in the calculations where increased phosphoryl protonation results in shorter, stronger N′−P bonds and protonation at the unsubstituted N″ nitrogen leads to longer, weaker N′−P bonds.

Comparing structures isoprotonic at the guanidinium group, we find that increasing protonation at the phosphoryl group leads to shorter N′−P bonds, where **2a** > **2b** > **2c** and **3a** > **3b** > **3c** (Table 1, Figure 4). Even for tetrahedral N′, structures **1b** and **1c** showed similar N′−P bond length trends where **1b** > **1c**. This is true at all levels of theory tested (Table 1). From a qualitative perspective, these results clearly show that decreased phosphoryl resonance leads to shorter N′−P bonds, as expected.[23,24,27]

The increase in N′−P bond lengths is strongly correlated to the total magnitude of N′−P bond-weakening n(O) → σ^*(N′−P) interactions. The correlation holds regardless of method used (Tables S3, S4, S5 and Figures S1 and S2, in the Supporting Information, and Figures 6 and 7) or the presence of solvation (Figure 7). R^2 values exceed 0.9 in all cases. To check that the correlations were correct and that the interactions were not anticooperative, an NBO deletion analysis comparing the total *E*(2) energy values to the simultaneously deleted interactions[68,71,79−83] was performed. With all structures, there is a slight positive cooperativity (Table S3 in the Supporting Information). Nevertheless, the correlation between the total n(O) → σ^*(N′−P) energy terms and N′−P bond lengths made does not change whether *E*(2) or deletion energies are used (Figure 6). The correlation of the simultaneously deleted energies with the N′−P bond lengths is insignificantly better with $R^2 = 0.989$ compared to $R^2 = 0.988$ for the sum of the *E*(2) values. Due to the insensitivity of the computed values to changes in solvent and method, *E*(2) values at the B3LYP/6-311++G(d,p)//B3LYP/6-311++G(d,p) level in vacuum are discussed throughout the manuscript.

(79) Brunck, T. K.; Weinhold, F. *J. Am. Chem. Soc.* **1979**, *101*, 1700.
(80) Foster, J. P.; Weinhold, F. *J. Am. Chem. Soc.* **1980**, *102*, 7211.
(81) Flores, J. R.; Estevez, C. M.; Carballeira, L.; Juste, I. P. *J. Phys. Chem. A.* **2001**, *105* (19), 4716−4725; **2001**, *105*, 4716.
(82) Belair, S. D.; Hernandez, H.; Francisco, J. S. *J. Am. Chem. Soc.* **2004**, *126*, 3024.
(83) Ulic, S. E.; Oberhammer, H. *J. Phys. Chem. A* **2004**, *108*, 1844.

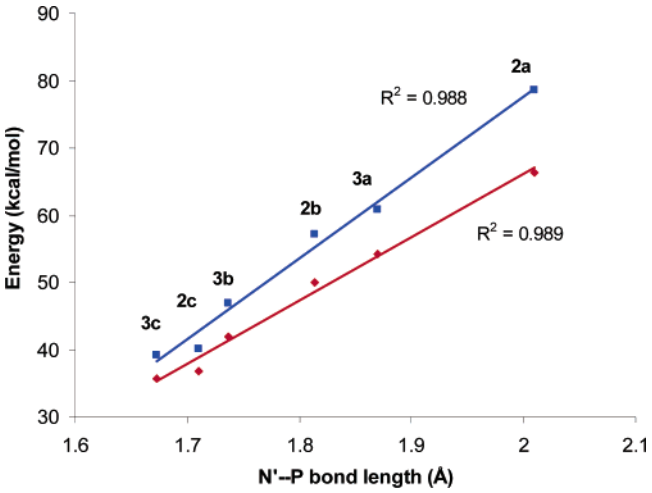

Figure 6. Graph showing the correlation between the energy values of the interactions of the n(O) → σ^*(N′−P) type with N′−P bond lengths using energies (red line) deleted simultaneously and the sum of the $E(2)$ energies (blue line). The level of theory used here is HF/6-311++G(d,p)//B3LYP/6-311++G(d,p).

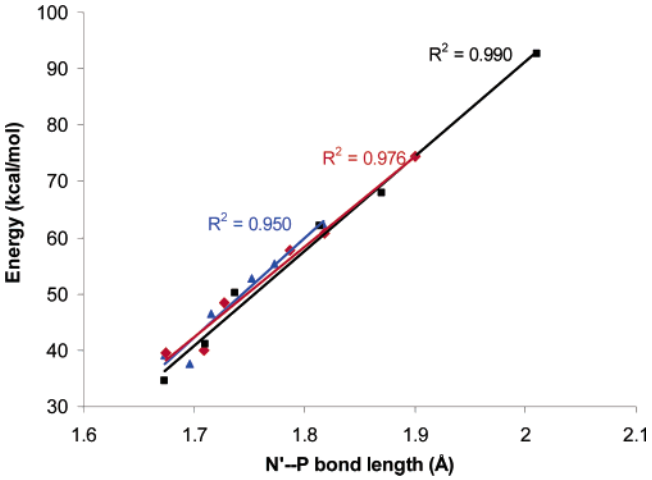

Figure 7. Graph showing the correlation between the energy values of the interactions of the n(O) → σ^*(N′−P) type with N′−P bond at the B3LYP/6-311++G(d,p)//B3LYP/6-311++G(d,p) level. The black line shows the gas-phase correlation, the red line at a dielectric of 2.379, and the blue line at a dielectric of 78.39. Each set (gas phase, dielectric = 2.379, and dielectric = 78.39) include, in ascending order of bond lengths, structures **3c**, **2c**, **3b**, **2b**, **3a**, and **2a**.

The sum of the interactions is presented. This is comprised of three reinforcing n(O) → σ^*(N′−P) interactions from each of the three phosphoryl oxygen atoms (six to eight lone pairs). The individual contribution from each interaction is approximately 20−30 kcal/mol when fully deprotonated (**1a**−**3a**). Our computed values are consistent with other n → σ^* values that have been previously published.[84,85]

The n(O) → σ^*(N′−P) interaction (Figure 8) is a generalized anomeric interaction of the Lp−X−A−Y variety where "Lp" represents a lone pair, "X", any heteroatom, "A" an electropositive atom, and "Y" and electronegative atom.[70,71,84,85] The generalized anomeric effect has been well documented as being responsible for a wide variety of effects most notably in molecular conformation.[86−88]

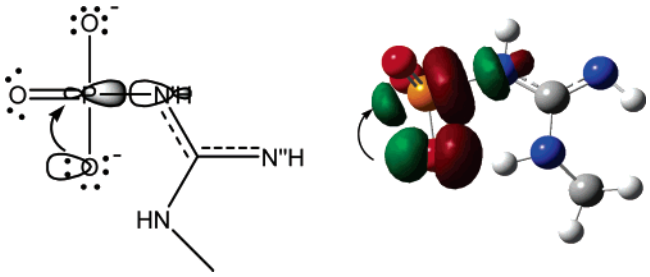

Figure 8. Schematic and orbital diagram of the anomeric interaction in **3a** between n(O) and σ^*(N′−P).

The computations provide an explanation on why increased phosphoryl protonation results in shorter N′−P bonds. A phosphoryl group has three lone pairs on each of the two negatively charged oxygen atoms and two lone pairs on the neutral oxygen atom (Figure 8). Successive protonation removes lone pairs of electrons from a possible anomeric interaction. The anomeric effect is further reduced by increasing the energy difference between the average n(O) lone pair energy and σ^*(N′−P), as shown in Table S6 in the Supporting Information. As protonation at the phosphoryl group increases (**2a** < **2b** < **2c** and **3a** < **3b** < **3c**) so does the n(O) → σ^*(N′−P) energy difference (**2a** < **2b** < **2c** and **3a** < **3b** < **3c**).

As discussed, protonation of the phosphoryl group modulates the number and quality of the n(O) → σ^*(N′−P) anomeric interactions, which is the primary factor in determining the N′−P bond length. Structure **2a** has the same phosphoryl protonation state as that of **3a**, **2b** as **3b**, and **2c** as **3c**. Therefore, it is expected that the magnitude of n(O) → σ^*(N′−P) should be equal for the pairs of structures **3a** and **2a**, **3b** and **2b**, and similarly **3c** and **2c**. The secondary factor found involves the guanidinium protonation state. Consider structures from series **2**, which are protonated at N″ to give a delocalized guanidinium. As such, N′ becomes more sp^2-like for structures **2a**−**2c** compared to structures **3a**−**3c**. The change in hybridization of N′ stabilizes the σ^*(N′−P) orbital allowing for more efficient overlap with n(O) lone pairs yielding a stronger anomeric effect for series **3**. This is seen in Table S6 in the Supporting Information, where the difference in energies between the average lone pair energy and σ^*(N′−P) is less in series **2** compared to series **3** (**2a** < **3a**, **2b** < **3b**, and **2c** < **3c**). Therefore, the protonation state changes for both series **2** and **3** are related and have the same influence on the anomeric effect giving a linear response.

The ranking of the N′−P bond lengths is as expected with the primary (phosphoryl protonation) and secondary (guanidinium protonation) factors in operation, **3c** < **2c** < **3b** < **2b** < **3a** < **2a**. Structure **3c** has the shortest N′−P bond, since the phosphoryl group is fully protonated and the guanidinium is not protonated, minimizing the anomeric effect. Structure **2c** has the second shortest N′−P bond, since with the same phosphoryl protonation state, the N″ guanidinium is protonated increasing the anomeric interaction. The pattern continues through all six structures.

The results explain why a stationary point could not be located for structure **2a** at the higher levels of theory. We find a large

(84) Hetenyi, A.; Martinek, T. A.; Lazar, L.; Zalan, Z.; Fulop, F. *J. Org. Chem.* **2003**, *68*, 5705.
(85) Kirby, A. J. *The Anomeric Effect and Related Stereoelectronic Effects at Oxygen*; Springer-Verlag: Berlin, 1983.
(86) Cao, X.; Hamers, R. J. *J. Am. Chem. Soc.* **2001**, *123*, 10988.
(87) Tao, F.; Lai, Y. H.; Xu, G. Q. *Langmuir* **2004**, *20*, 366.
(88) Kadossov, E. B.; Rajasekar, P.; Materer, N. F. *J. Phys. Chem. B* **2004**, *108*, 303.

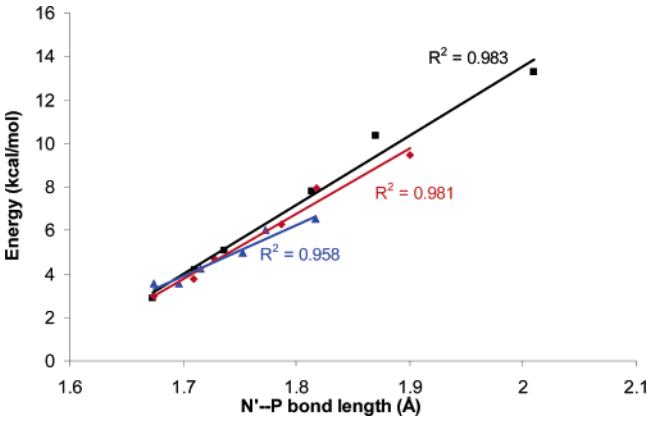

Figure 9. Correlation between N′−P bond lengths and the sum of the σ(N′−P) → σ*(C−N) and σ(N′−P) → σ*(C−N″) interaction energies at the B3LYP/6-311++G(d,p)//B3LYP/6-311++G(d,p) level. The black line shows the gas-phase correlation, the red line shows the correlation at a dielectric of 2.379, and the blue line shows the correlation at a dielectric of 78.39. Each set (gas phase, dielectric = 2.379, and dielectric = 78.39) include, in ascending order of bond lengths, structures **3c**, **2c**, **3b**, **2b**, **3a**, and **2a**.

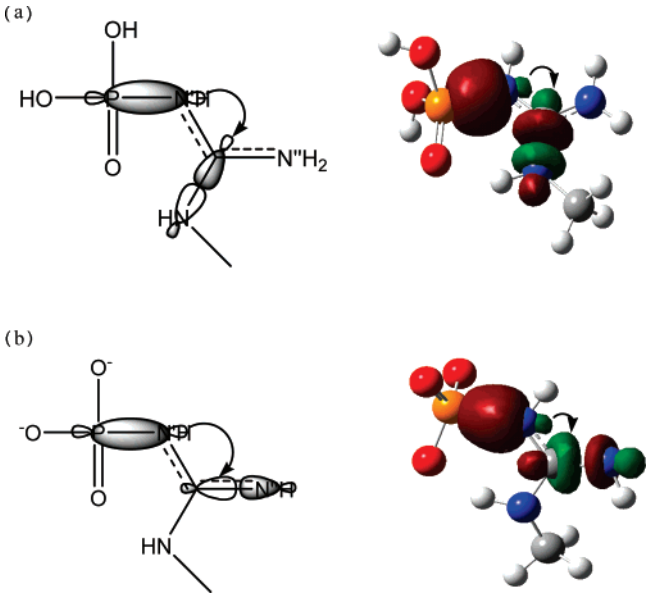

Figure 10. Stereoelectronic interactions (a) σ(N′−P) → σ*(C−N) in **2c** and (b) σ(N′−P) → σ*(C−N″) in **3a**.

n(O) → σ*(N′−P) energy interaction for structure **2a**. It is possible that the N′−P bond fails to form in **2a** at the MP2/6-311++G(d,p) level, because of the bond-weakening anomeric interaction. The lower levels of theory may not have properly described this phenomenon and produced a stationary point.

Role of the N−P Bond as a Donor: Interactions with Guanidinium. Comparing structures that are isoprotonic at the phosphoryl group, but either singly or doubly protonated at N″, we find in terms of N′−P bond lengths that **2a** > **3a**, **2b** > **3b**, and **2c** > **3c** (Table 1, Figure 4). Doubly protonated N″ forms display longer N′−P bond lengths. Again this is true at all levels of theory. Any nitrogen atom on a guanidinium group with only one proton effectively locks the lone pair on that nitrogen into a double C=N bond, preventing it from participating in delocalization interactions involving the guanidinium group. Two protons on N″ makes it more sp^3-like, allowing more conformational freedom and possible delocalization with the guanidinium system.

The NBO results also show σ(N′−P) → σ*(C−N) and σ(N′−P) → σ*(C−N″) interactions that could contribute to the weakening of the N′−P bond (Figures 9 and 10). The total magnitude of the N′−P bond-weakening interactions are correlated with N′−P bond lengths. The E(2) and Edel magnitudes are **2a** > **3a**, **2b** > **3b**, and **2c** > **3c** mirroring differences in N′−P bond lengths (Tables S4 and S5 in the Supporting Information and Figure 9). This can be rationalized by the fact that deprotonation of N″ locks the lone pair on N″ into a double bond at C=N″ making it difficult for other delocalized forms to exist[54] in series **3** structures relative to series **2**. As the N′−P bond is a source of electrons for guanidinium delocalization, it is lengthened as it is weakened with increasing σ(N′−P) → σ*(C−N) and σ(N′−P) → σ*(C−N″) interactions in series **2**. The correlation (R^2 = 0.994) between the sum of σ(N′−P) → σ*(C−N) and σ(N′−P) → σ*(C−N″) interactions and N′−P bond lengths is clear, but these stabilizing interactions are weaker than the generalized anomeric interaction n(O) → σ*(N′−P) previously discussed.

Being of the same protonation state at the guanidinium, **2a**, **2b**, and **2c** as well as **3a**, **3b**, and **3c** are expected to have almost equal σ(N′−P) → σ*(C−N) and σ(N′−P) → σ*(C−N″) interactions. The fact that the σ(N′−P) → σ*(C−N) and σ(N′−P) → σ*(C−N″) interactions decrease in order of **2a** > **2b** > **2c** and **3a** > **3b** > **3c** according to N′−P bond lengths may be explained by a better overlap between the σ(N′−P) and σ*(C−N) and σ*(C−N″) orbitals and stronger stereoelectronic effect in forms with less protonation at the phosphoryl group, as shown in Table S7 in the Supporting Information. The trend in the energy difference between the σ(N′−P) and σ*(C−N) and σ*(C−N″) is **2a** < **2b** < **2c** and **3a** < **3b** < **3c**, thus explaining the linearity seen for all structures in Figure 9.

***N*-Methyl-*N*′-phosphorylguanidine with a Quaternary Nitrogen at N′.** The calculations indicate that when N′ is quaternary, the N′−P bond is weakened. Structures **1b** and **1c** both show a quaternary nitrogen at the N′ position. The N′−P bonds of **1b** and **1c** are longer than their isoprotonic counterparts **2b** and **2c** that have ternary N′ nitrogens, as shown in Table 1. The N′−P bonds of **1b** and **1c** are also longer than in their counterparts **3b** and **3c** that have a ternary N′ nitrogen. The increase in the N′−P bond length suggests that the N′−P is weaker if the N′ is quaternary.

NBO analysis shows that as expected the anomeric n(O) → σ*(N′−P) interaction is greater in **1b** than **1c** with interaction energies, E(2), values of 139.1 kcal/mol and 70.8 kcal/mol, respectively for the B3LYP/6-311++G(d,p)-optimized structures. For the MP2/6-311++G(d,p)-optimized structures, this value is 137.4 and 76.9 kcal/mol, respectively. Because the values of the anomeric n(O) → σ*(N′−P) interaction are well correlated to N′−P bond lengths, we expect that the E(2) values for the same interaction to be even larger for structure **1a**. To test this and because we were unable to find a minimum structure for **1a** at any theory level tested, we performed an NBO analysis on minimized structures for **1b** with the extra proton on the phosphoryl removed. While not a true stationary point, this calculation provides an idea of the magnitude of the anomeric n(O) → σ*(N′−P) interaction. We have found for both the MP2/6-311++G(d,p) and B3LYP/6-311++G(d,p) structures, the anomeric n(O) → σ*(N′−P) interactions are increased

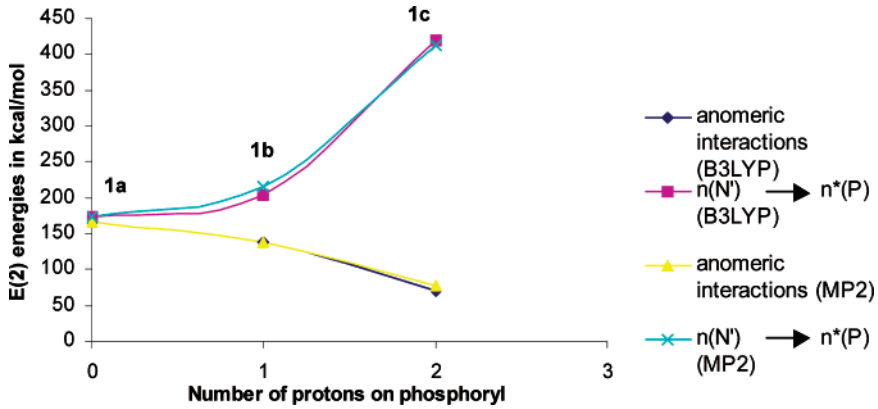

Figure 11. Interaction energies for series **1** structures. For structure **1a**, when the N′−P bond does not form, the anomeric interactions, i.e., the n(O) → n*(N′−P) interactions that favor breaking the N′−P bond, are almost equal to the n(N′) → n*(P) interactions that favor forming the N′−P bond. When the N′−P bond is shorter and stronger, the n(N′) → n*(P) interaction (that favors forming the N′−P bond) dominates. *E*(2) interaction energies are used in this case.

for this restrained structure, **1a**, with values of 167.0 kcal/mol for both structures explaining its instability.

Dative bonds formed from a nitrogen lone pair as a donor are well documented in the literature,[89,90] as well as those with phosphorus as an acceptor.[6] Our calculations show that this dative interaction, seen by n(N) → n*(P) energies, may provide an explanation of the dissociation of **1a**. In structures with longer N′−P bonds, lesser dative n(N) → n*(P) interactions are expected. The NBO analysis supports such an interpretation where the n(N) → n*(P) interactions increase with shorter N′−P bond lengths. For example, the *E*(2) values for the n(N) → n*(P) interactions at the B3LYP/6-311++G(d,p) level increase from 173.7 kcal/mol to 203.2 kcal/mol to 419.4 kcal/mol from **1a** to **1b** to **1c**. At the MP2/6-311++G(d,p) level these values are 173.7, 216.0, and 411.6 kcal/mol. Taken together (Figure 11) the dissociation of the N′−P bond in **1a** occurs when the magnitude of the n(N) → n*(P) bond stabilizing interaction is no greater than the anomeric n(O) → σ*(N′−P) destabilizing interactions. Bond formation will occur if the dative forces are greater than the destabilizing anomeric effect, explaining why structure **1a** is not a stationary point.

Opposing Resonance Theory. The opposing resonance theory states that the weakness of the N′−P bond is due to the competition for the same lone pair on N′ by two strongly delocalized groups, i.e., phosphoryl and guanidinium. For opposing resonance to be a significant effect, the magnitude of the delocalization of the lone pair on N′ toward the guanidinium should be approximately equal to the delocalization of the same lone pair toward the phosphoryl group. In short, the magnitude of the n(N′) → σ*(C−N) and n(N′) → σ*(C−N″) interactions should be nearly equal to that of the n(N′) → σ*(P−O) type interactions. However, for all structures, the magnitude of n(N′) interactions with C−N and C−N″ bonds are markedly greater than those with P−O bonds (Tables S8 and S9 in the Supporting Information). As expected, this imbalance toward the guanidinium gives little competition for the lone pair, and opposing resonance is not a strong effect.

To support opposing resonance theory, it is also expected that a balance of n(N′) → σ*(C−N″) and n(N′) → σ*(C−N) with n(N′) → σ*(P−O) interactions to be greater in structures with longer N′−P bonds. For example, the (N′) → σ*(C−N) and n(N′) → σ*(C−N″) interactions and the n(N′) → σ*(P−O) interactions should be larger and better balanced in **3a** than **3c**. Again the results show that this is not the case when comparing all structures (Tables S8 and S9 in the Supporting Information). For example, for structure **3a**, the values are 50.6 kcal/mol for the n(N′) → σ*(C−N) and n(N′) → σ*(C−N″) interactions compared to 7.2 kcal/mol for the n(N′) → σ*(P−O) interactions. For structure **3c**, the values are 27.5 kcal/mol for the n(N′) → σ*(C−N) and n(N′) → σ*(C−N″) interactions compared to 23.6 kcal/mol for the n(N′) → σ*(P−O) interactions. In fact, this is opposite to opposing resonance theory with the structure with the shorter N′−P bond experiencing more competition for the lone pair of N′ and therefore less overall resonance than the structure with the longer N′−P bond.

In fact no relationship between the n(N′) → σ*(C−N) and n(N′) → σ*(C−N″) as well as n(N′) → σ*(P−O) interactions and N′−P bond lengths can be derived from the interaction energies (Tables S8 and S9 in the Supporting Information). The computed data underscores the inability of opposing resonance theory to describe N′−P bond lability in phosphagens.

Relevance to High-Energy Phosphoryl Bonds. The lability of "high-energy" phosphoryl bonds is crucial for many cellular processes, in particular, cellular energy buffering by phosphagens and energy production by ATP hydrolysis.[23,24] However, detailed structural studies have been limited due to the lability of these "high-energy" bonds possibly from experimental resolution and time scale issues. In modern textbooks,[23,24] a qualitative understanding based upon the opposing resonance effect, resonance stabilization, and solvation have been used to explain this phenomenon. For the first time, we have shown that the anomeric effect plays a significant role in the weakness of the N′−P bond and not the opposing resonance effect. The anomeric effect also explains the trend that increasing phosphoryl resonance leads to longer N′−P bonds. The symmetry between the phosphate groups in ATP could imply a more balanced competition for the lone pair on the bridging oxygen atom, giving a more significant opposing resonance effect. Nevertheless, the computed evidence of the significant role the

(89) Kobayashi, J.; Goto, K.; Kawashima, T. *J. Am. Chem. Soc.* **2001**, *123*, 3387.
(90) Kobayashi, J.; Goto, K.; Kawashima, T.; Schmidt, M. W.; Nagase, S. *J. Am. Chem. Soc.* **2002**, *124*, 3703.
(91) Scott, A. P.; Radom, L. *J. Chem. Phys.* **1996**, *100*, 16502.

anomeric effect plays in weakening the N′−P bond in phosphagens requires such reinforcing anomeric effects to be considered in the lability of the O−P bond in ATP. In particular, the anomeric control of "high-energy" bonds is likely to impact the understanding of phosphoryl transfer reaction mechanism and catalysis.

Conclusion

Modulating the resonance capability of *N*-methyl-*N*′-phosphorylguanidines by studying structures differing in both the number and placement of protons provides a novel interpretation of the stereoelectronic factors contributing to the lability of the "high-energy" N′−P bond in phosphagens. Compelling evidence shows that decreased delocalization at either the phosphoryl or guanidinium groups of *N*-methyl-*N*′-phosphorylguanidine results in stronger N′−P bonds in accordance with the traditional view that the phosphoryl and guanidinium are more strongly stabilized by resonance when separated than when bonded. In particular, an explicit link between different protonation states and N′−P bond lengths is provided by the quantum computations. For example, protonation at N″ alone is sufficient to cause significant weakening of the N′−P bond. However, evidence of competition between the phosphoryl and guanidinium groups for the same lone pair on the bridging nitrogen, N′, is not found as described in opposing resonance theory. Indeed, we find that interactions between the lone pair on the bridging nitrogen, N′, and the guanidinium dominates over interactions between the same lone pair and the phosphoryl thus negating the possibility of competition between the two groups. The weakness of the N′−P bond is directly correlated with an increase in the anomeric interaction n(O) → σ^*(N′−P). To a lesser extent, interactions of σ(N′−P) → σ^*(C−N) and σ(N′−P) → σ^*(C−N″) type can also explain the weakness of the N′−P bond. These interactions directly correlate N′−P bond strength with protonation state and provide a rationalization for an increase in overall resonance being accompanied by a weakening of the N′−P bond. The anomeric effect in particular provides an intriguing new avenue into the factors controlling the strength of "high-energy" bonds and phosphoryl transfer reactions.

Acknowledgment. This work was funded in part by an American Heart Association (Florida, Puerto Rico affiliate) predoctoral fellowship (0415212B) to E.A.R. In addition, J.D.E. is grateful to the NSF (CHE-0321147, CHE-0354052, AAB/PSC CHE-030008P), Department of Education (P116Z040100 and P116Z050331), and IBM and SGI Corporations for the support of this work. The authors thank the FSU School of Computational Science and Information Technology (CSIT) for use of the IBM p-Series 690 Power3-based supercomputer and the IBM p-Series 690 Power4-based supercomputer.

Supporting Information Available: Gaussian archives for all eight structures at B3LYP/6-311++G(d,p) and MP2/6-311++G(d,p); second-order interaction energies (B3LYP/6-311++G(d,p) and MP2/6-311++G(d,p)) for all eight structures; selected bond lengths at all theory levels, Table S1; absolute energies, Table S2; simultaneously deleted energies and *E*(2) energies, Table S3; anomeric, n(O) → σ^*(N′−P) and σ(N′−P) → σ^*(C−N) and σ(N′−P) → σ^*(C−N″) interactions (B3LYP/6-311++G(d,p)), Table S4; anomeric, n(O) → σ^*(N′−P) and σ(N′−P) → σ^*(C−N) and σ(N′−P) → σ^*(C−N″) interactions (MP2/6-311++G(d,p)), Table S5; energy values of the oxygen lone pairs and σ^*(N′−P), Table S6; energy values of σ(N′−P) and σ^*(C−N) as well as σ^*(C−N″), Table S7; N′ lone pair interactions (B3LYP/6-311++G(d,p)), Table S8; N′ lone pair interactions (MP2/6-311++G(d,p)), Table S9; complete references for 23 and 24; Figure S1, anomeric, n(O) → σ^*(N′−P) energies vs N′−P bond lengths at different theory levels; Figure S2, σ(N′−P) → σ^*(C−N) and σ(N′−P) → σ^*(C−N″) interactions vs N′−P bond lengths at different theory levels. This material is available free of charge via the Internet at http://pubs.acs.org.

JA054708V